On Sloshing Effects of Liquid in Cylindrical and Spherical Vessels during a Strong Earthquake

by Kiyoshi SOGABE[I]

SYNOPSIS

Earthquake response observation of the cylindrical storage by a large scale model, response analysis of sloshing of liquid in the cylindrical storage and the response analysis of sloshing of liquid in the spherical storage were carried out to make clear the fundamental vibrational characteristics of cylindrical and spherical storages. These are reported in this paper. The results are illustrated into charts which are available for the response calculation of sloshing of liquid in the aseismic design of cylindrical and spherical storages.

I) Graduate Student, University of Tokyo

1. Introduction

In the aseismic design of a liquid storage up to this time, its stability was the only item checking by law to consider the possibility of its overturn by a certain level of horizontal seismic force. After that, the more the technique of dynamic analysis became to be adopted in the aseismic design of structure, the more in the aseismic design of liquid storage. However, the response analysis now in use for the aseismic design of liquid storage is based on the acceleration records of strong earthquakes as for the aseismic design of structure. The effect of the component of long period is completely omitted to analyze the sloshing of liquid in the acceleration record. Furthermore, the fundamental vibrational characteristics of spherical storage are not well known.

The author carried out a series of experiment and analyses to make clear the fundamental characteristics of sloshing effects of liquid in cylindrical and spherical storages. In this paper, the author will report on next three items.

1) Earthquake response observation of the cylindrical storage by a large scale model.
2) Response analysis of sloshing of liquid in the cylindrical storage.
3) Response analysis of sloshing of liquid in the spherical storage.

2. Earthquake Response Observation of the Cylindrical Storage by a Large Scale Model

2.1 Outline of the Response Observation

An experiment of observation was carried out to know the response of cylindrical storage during natural earthquakes.

The objects of this experiment are next two points.

1) To observe the displacement of the ground motion in order to obtain the records of earthquake motion as input waves for the analysis.
2) To observe the response of the vessel and the surface of liquid during natural earthquakes by using a large scale cylindrical storage model which is similar to the storage now in use.

In this experiment, the dimension of the model storage was decided to set the natural period of sloshing of liquid close to the dominant period of the displacement of the ground motion. The model tank was decided to be settled in a place of Chiba Field Station, the Institute of Industrial Science, University of Tokyo.

Through the result of earthquake observation, the dominant periods of the displacement of the ground motion T_g are identified as 2.3 sec , 3.6 sec and 9.4 sec in the region from 1 sec to 10 sec . So the dimension of model storage was decided to set the natural period of sloshing of liquid T_1 close to a dominant period T_g = 2.3 sec . This is given as follows.

Diameter: $D = 4.0\,m$
Height of Side Wall: $H_w = 1.8\,m$

In this case, the period of sloshing of liquid T_1 changes according to the height of liquid H. The relation between H and T_1 is shown in Fig. 1.

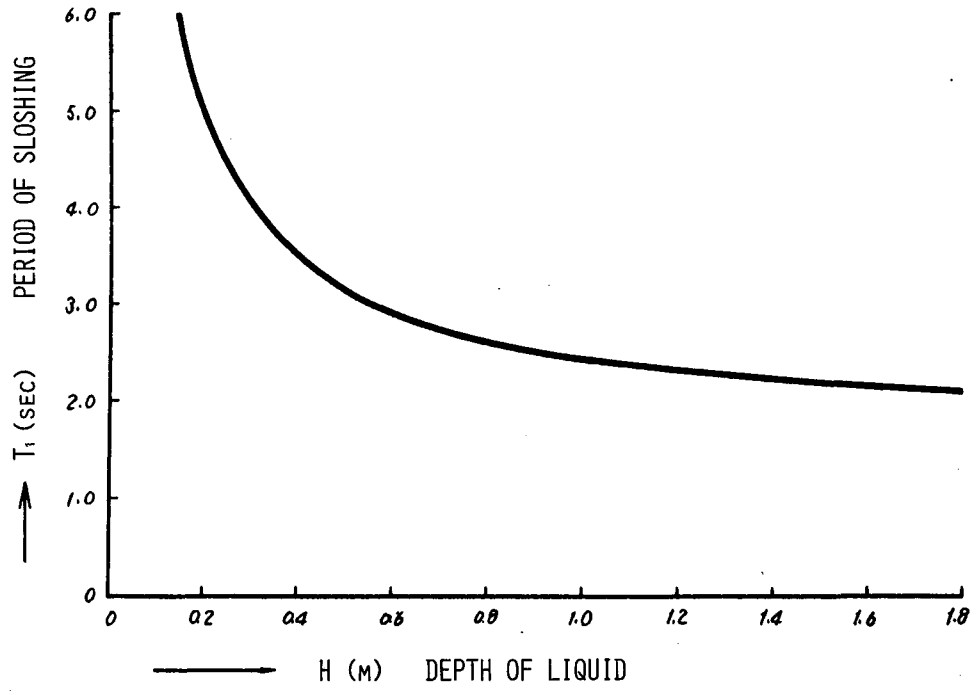

Fig. 1 Period of Sloshing of Liquid in the Storage Model

It is obtained from this figure that the depth of liquid should be 1.6 m so as to the period of sloshing of liquid T_1 is equal to the dominant period T_g.

The observation was carried out for NS component of the ground displacement, NS component of the ground acceleration, sloshing displacements of liquid surface at two points on a diameter, pressures at two points of side wall and strains at two points of the vessel.

To observe the ground displacement and ground acceleration, pick-ups were set on the concrete block of 1m x 1m x 1m, which was isolated from the concrete floor of the building (cf. Fig. 2). The items of observation and their symbols for the ground motion in this paper is as follows.

1) ACC: Acceleration of the ground motion (in NS)
2) DISP: Displacement of the ground motion (in NS)

The storage model was settled on the concrete base whose diameter was 6.0m and thickness 0.6m (cf. Fig. 3).

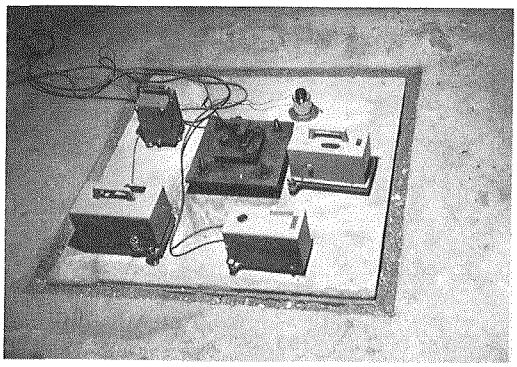

Fig. 2 Pick-ups on the Concrete Block

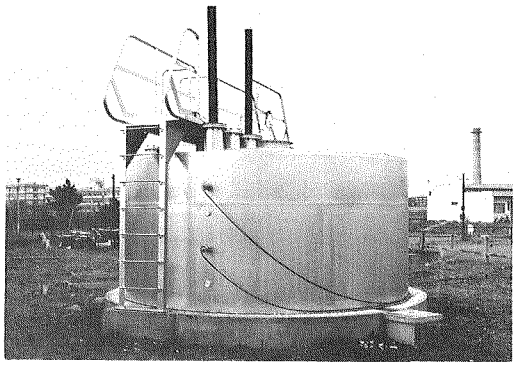

Fig. 3 Storage Model

Six items were observed on the model storage to know its response (cf. Fig. 4). The items of observation and their symbols for the model storage are as follows.

3) SL1: Displacement of sloshing of liquid (outer point)
4) SL2: Displacement of sloshing of liquid (inner point)
5) PR1: Pressure at side wall (upper point)
6) PR2: Pressure at side wall (lower point)
7) ST1: Strain of the vessel (upper point)
8) ST2: Strain of the Vessel (lower point)

The detail of the model storage is shown in Fig. 5.

The recording of its response was controlled by the starter. The starter was set to start its recording when the pick up for the starter felt the acceleration more than 0.5 gal. The pick up for the starter was set on the same concrete block on which the pick ups for ground acceleration and ground displacement were set. By this method, when a earthquake wave arrived, the operation of oscillograph was continued for 6 min. The system for measurement and recording is shown in Fig. 6.

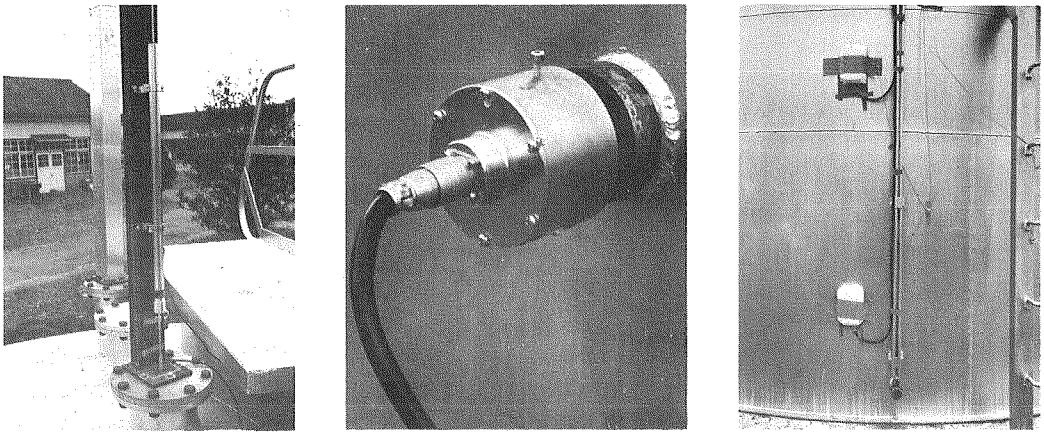

Displacement of Free Surface of Liquid

Pressure at Side Wall

Strain of the Vessel

Fig. 4 Pick-ups to Measure the Response of the Storage

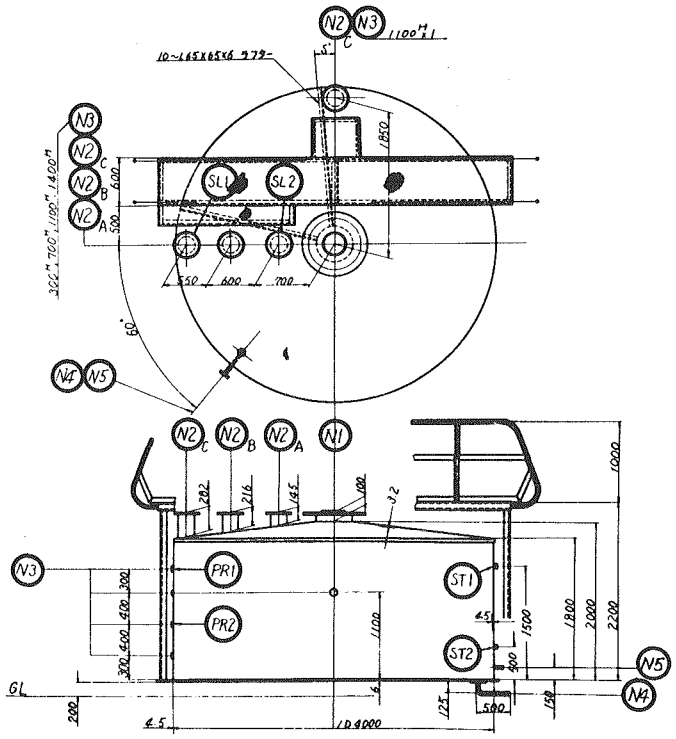

Fig. 5 Dimension of the Model Storage

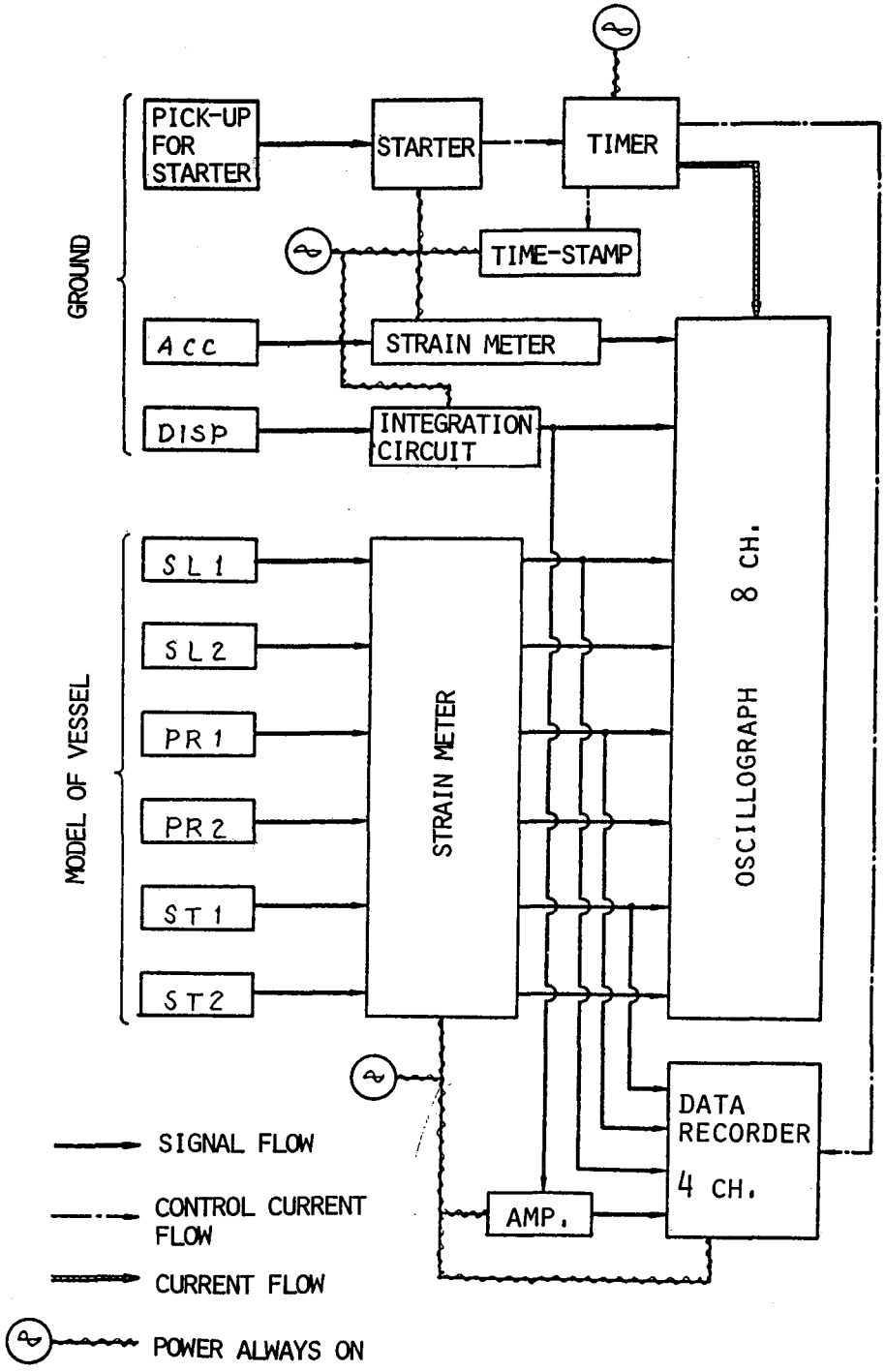

Fig. 6 System for Measurement and Recording

2.2 Result of Observation

About 50 records of observation were obtained from Jan. 1973 to Nov. 1975. First, these records were classified as shown in Fig. 7 by the location of their epicenter.

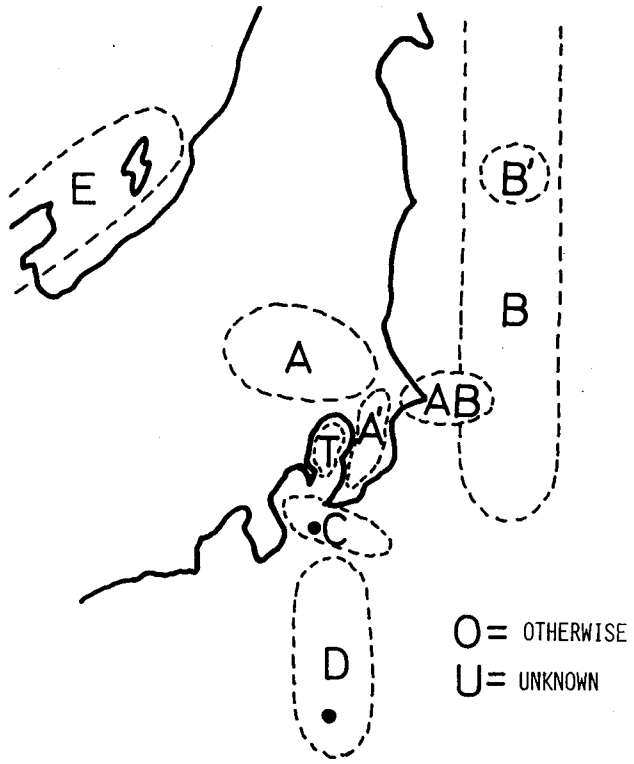

Fig. 7 Location of Epicenter

Next, the records were classified and analyzed as follows.

2.2.1 Classification of the Response

It was found, by the inspection for the records, that the responses of the liquid storage are classified into next three types.

1) Acceleration type response (cf. Fig. 8):
The response whose wave is similar to the acceleration of the ground motion. In this response, the maximum value of response is given at the time close to that of the acceleration of the ground motion. This response is

called acceleration type response because it is thought that the liquid storage responses in wide frequency range to the frequency component of the acceleration of the ground motion.

2) Displacement type response (cf. Fig. 9):
The response whose wave is similar to the wave of displacement of the ground motion. In this response, the maximum value of response is given rather later than that of the acceleration of the ground motion. This response is called displacement type response because it is thought that the liquid storage responses resonantly to the frequency component of the displacement of the ground motion. It was found that the ground displacement wave which causes the response of this type is similar to sinusoidal wave and that the response waves of the storage is also similar to sinusoidal wave.

3) Mixed type response (cf. Fig. 10):
The response which shows acceleration type response in its early time but displacement type response in its later time and gives the same order maximum value in both types of response.

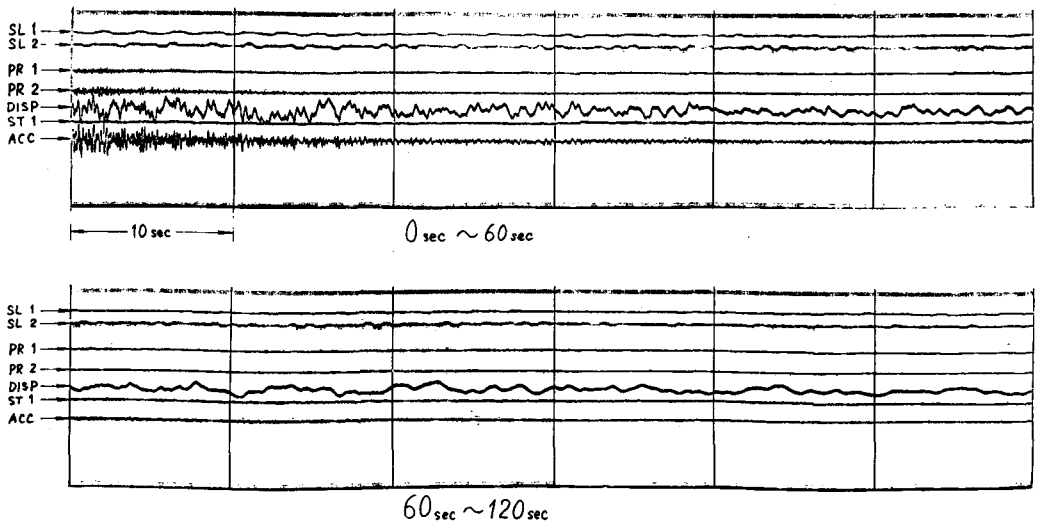

Fig. 8 Response of Acceleration Type

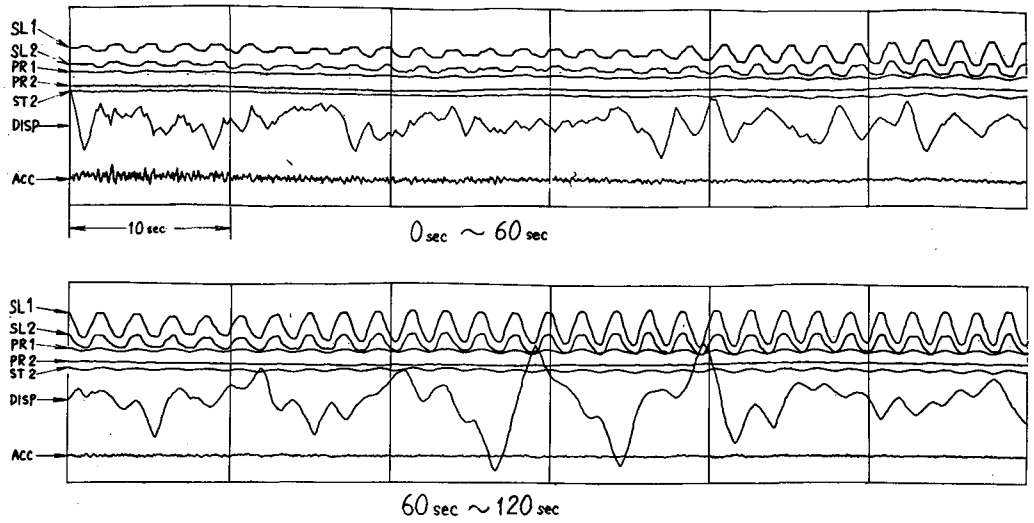

Fig. 9 Response of Displacement Type

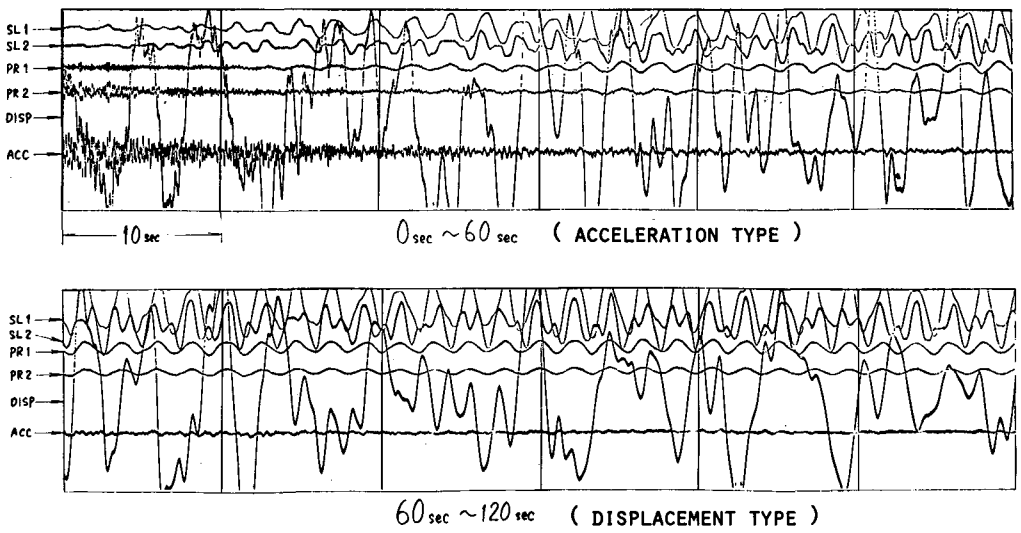

Fig. 10 Response of Mixed Type

2.2.2 Acceleration and Displacement of the Ground Motion

Fig. 11 represents the relation between the maximum acceleration of the ground motion and the distance of epicenter. This shows that the longer the distance of epicenter, the smaller the maximum acceleration of the ground motion.

Fig. 12 represents the relation between the maximum displacement of the ground motion and the distance of epicenter. This shows that the longer the distance of epicenter, the larger the displacement of the ground motion.

Fig. 13 represents the relation between the maximum displacement of the ground motion and the maximum acceleration of the ground motion. This shows that the larger the maximum acceleration of the ground motion, the larger the maximum displacement of the ground motion. This also shows that, if the value of the maximum acceleration of the ground motion is the same order value, the maximum displacements of the ground during earthquakes which have their epicenter in the ocean (B, B' etc.) are larger than those during earthquakes which have their epicenter in the land (A, A' etc.).

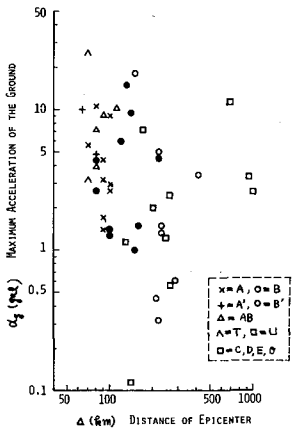

Fig. 11

Relation between the Distance of Epicenter and the Maximum Acceleration of the Ground

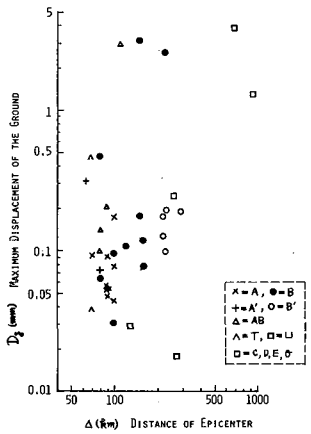

Fig. 12

Relation between the Distance of Epicenter and the Maximum Displacement of the Ground

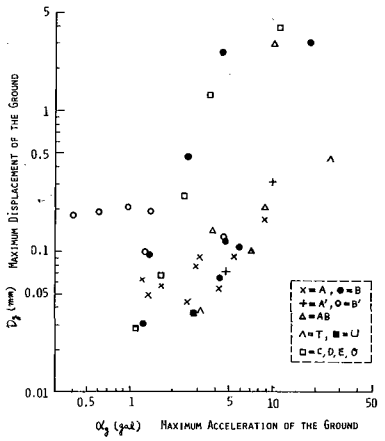

Fig. 13

Relation between the Maximum Acceleration of the Ground and the Maximum Displacement of the Ground

Fig. 14 represents an example of power spectrum of the ground displacement wave which caused the typical displacement type response. This shows that the dominant periods of the ground displacement T_g are 2.3 5 sec , 2.8 5 sec , 3.6 5 sec and 9.4 sec in the range from 1 sec to 10 sec . It is thought that the sloshing of liquid was caused mainly by the component of dominant period 2.3 5 sec , because the natural period of sloshing of liquid T_1 was 2.2 sec as mentioned before.

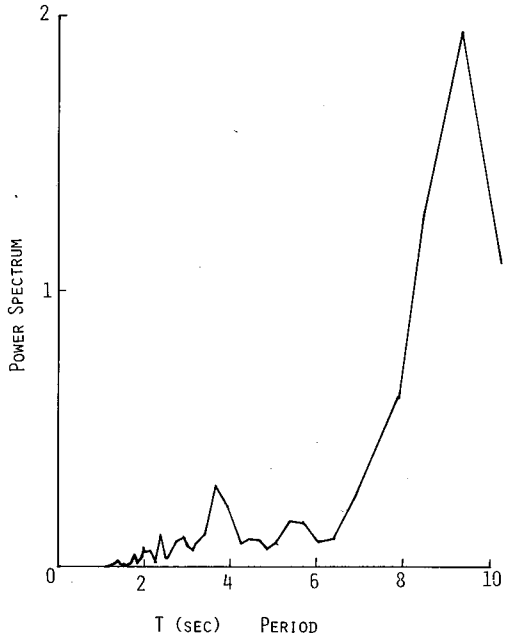

Fig. 14 Power Spectrum of the Displacement Wave of the Ground

2.2.3 Response of Liquid Storage

Fig. 15 represents the maximum response value of the liquid displacement h as the response factor h/α_g for acceleration type response and h/D_g for displacement type response. This shows that almost all the responses of the liquid displacement are the displacement type response and that the response values at the outer point (SL1) are larger than that at the inner point (SL2).

Fig. 16 represents the maximum response value of the side wall pressure p as the response factor p/α_g for acceleration type response and p/D_g for displacement type response. This shows that

there exist both type of responses but the acceleration type responses are more than displacement type responses. And this shows also that the response values at lower point (PR2) are larger than those at upper point (PR1) for the acceleration type response while the response values at upper point (PR1) are larger than those at lower point (PR2) for the displacement type response.

Fig. 17 represents the maximum response value of the side wall strain ε as the response factor ε/α_g for acceleration type response and ε/D_g for displacement type response. Though the number of data is very few, it may be shown that there exist both type of responses and that the response values at lower point (ST2) are always larger than that at upper point (ST1).

It may be obtained, from Figs. 15, 16, 17, that the dispersion of the response factor is rather large. The statistical values for each response factor were calculated. These are shown in Tab. 1.

This shows that, for liquid displacement and side wall pressure which have enough number of data for statistical calculation, the coefficients of variation of acceleration type response are larger than those of displacement type response.

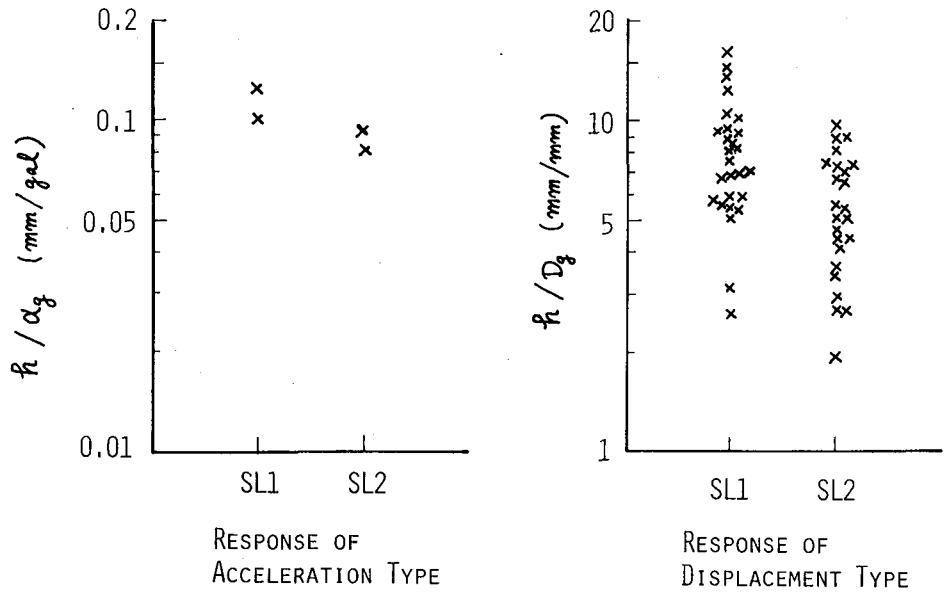

Fig. 15 Response of Displacement of Liquid Surface

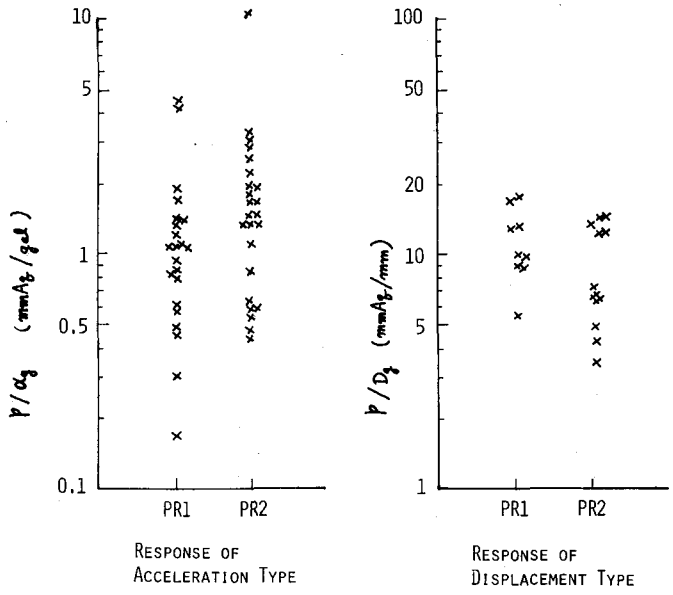

Fig. 16 Receponce of Pressure at Side Wall

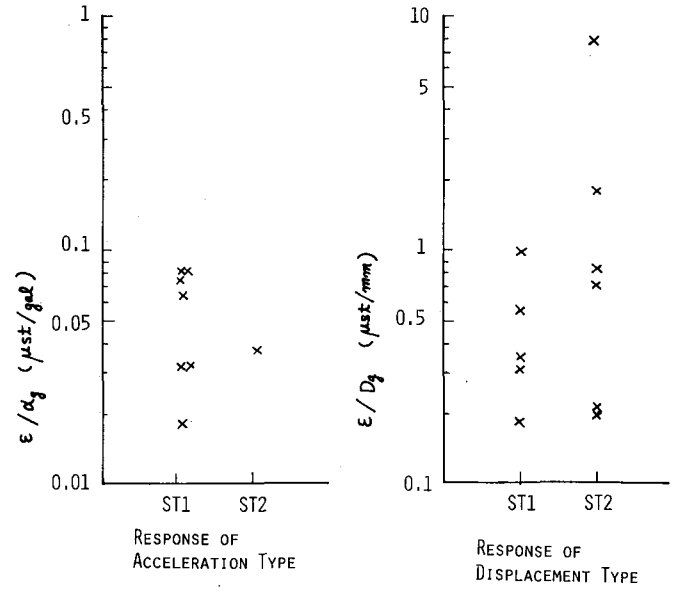

Fig. 17 Response of Strain of the Vessel

Tab. 1 Statistical values for each response factor

Items	Type of response	Symbol	Mean value	Standard deviation	Coefficient of variation
Displacement of liquid surface	Acc. type	SL1	0.0857 mm/gal	0.0452 mm/gal	0.527
		SL2	0.0766 mm/gal	0.0289 mm/gal	0.376
	Disp. type	SL1	8.25 mm/mm	3.37 mm/mm	0.409
		SL2	5.35 mm/mm	2.11 mm/mm	0.395
Side wall pressure	Acc. type	PR1	1.36 mmAq/gal	1.13 mmAq/gal	0.833
		PR2	1.98 mmAq/gal	2.05 mmAq/gal	1.04
	Disp. type	PR1	12.42 mmAq/mm	4.40 mmAq/mm	0.354
		PR2	10.2 mmAq/mm	4.61 mmAq/mm	0.453
Strain of vessel	Acc. type	ST1	0.0484 μst/gal	0.0288 μst/gal	0.595
		ST2	0.0383 μst/gal	——— μst/gal	———
	Disp. type	ST1	0.622 μst/mm	0.311 μst/mm	0.500
		ST2	3.45 μst/mm	3.86 μst/mm	1.12

3. Response Analysis of Sloshing of Liquid in a Cylindrical Storage

3.1 Basic Equations for Response Analysis

It is the object in this section to induce the basic equations to evaluate the sloshing effects of liquid in a cylindrical storage during the ground motion $d_g(t)$.

The analytical model of the cylindrical storage is illustrated in Fig. 18. The storage is assumed to be a rigid cylindrical vessel. R denotes the radius of the vessel and H the depth of liquid contained in it.

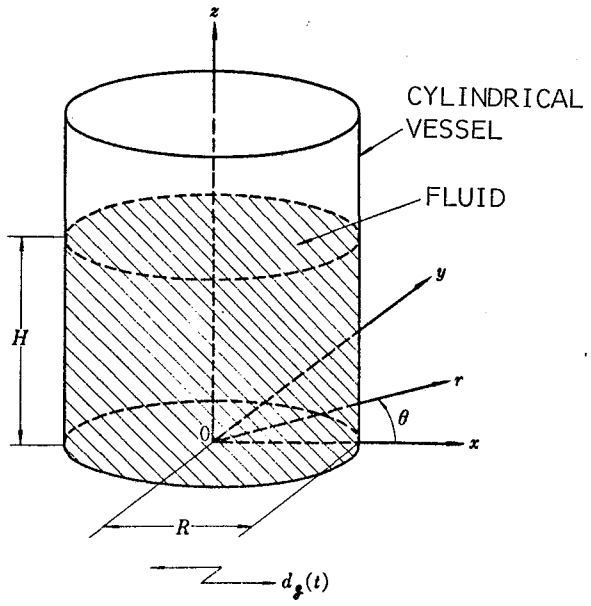

Fig. 18 Analytical Model

If it is assumed that the liquid is incompressive ideal fluid and irrotational, the velocity potential ϕ can be introduced. So the motion of liquid in the vessel is described by next four equations.

A) Continuity condition

$$\nabla^2 \phi = 0 \qquad (1)$$

B) Boundary Conditions

a) On the side wall

$$-\frac{\partial \phi}{\partial r}\bigg|_{r=R} = v_g \cos\theta\,, \quad v_g = \dot{d}_g \tag{2}$$

b) On the bottom

$$-\frac{\partial \phi}{\partial r}\bigg|_{z=0} = 0 \tag{3}$$

c) On free surface

$$\frac{\partial^2 \phi}{\partial t^2} + g\frac{\partial \phi}{\partial z} = 0 \;;\; z = H \tag{4}$$

Solving eqs. (1), (2), (3), (4), the velocity potential ϕ is obtained as follows.

$$\phi = R\left\{\sum_{i=1}^{\infty} \frac{2}{\varepsilon_i^2 - 1} \frac{J_1\left(\varepsilon_i \frac{r}{R}\right)}{J_1(\varepsilon_i)} \frac{\cosh\left(\varepsilon_i \frac{z}{R}\right)}{\cosh\left(\varepsilon_i \frac{H}{R}\right)} v_i - \frac{r}{R} v_g\right\} \cos\theta \tag{5}$$

where $J_1(r)$ denotes the Bessel function of the first order. ε_i denotes the i-th root of the equation $J_1'(\varepsilon)=0$, and is given in Tab. 2.

Tab. 2 Value of ε_i

i	ε_i	i	ε_i
1	1.841	6	18.015
2	5.331	7	21.165
3	8.536	8	24.311
4	11.706	9	27.457
5	14.863	10	30.602

The nominal velocity response of liquid v_i for each mode is given as the solution of next differential equation.

$$\ddot{v}_i + \omega_i^2 v_i = \ddot{\alpha}_g \tag{6}$$

where ω_i denotes the eigen frequency of sloshing of liquid of i-th order and is given as follows.

$$\omega_i = \sqrt{\frac{g}{R}\varepsilon_i \tanh\left(\varepsilon_i \frac{H}{R}\right)} \tag{7}$$

And α_g denotes the acceleration of the ground motion, that is

$$\alpha_g = \dot{v}_g = \ddot{d}_g$$

If the existence of damping is assumed for the motion of each mode, Eq. (6) can be modified into next form.

$$\ddot{v}_i + 2\zeta_i \omega_i \dot{v}_i + \omega_i^2 v_i = \ddot{\alpha}_g \tag{8}$$

where ζ_i denotes the damping coefficient. The eq. (8) is quite different from the response equation which is usually used for the ordinary dynamic analysis.

The response of the liquid surface displacement η is given as follow by using eq. (5).

$$\eta = \frac{1}{g} \frac{\partial \phi}{\partial t}\Bigg|_{z=H}$$

$$= R \frac{1}{g} \sum_{i=1}^{\infty} \frac{2}{\varepsilon_i^2 - 1} \frac{J_1(\varepsilon_i \frac{r}{R})}{J_1(\varepsilon_i)} (\alpha_i - \alpha_g) \cos\theta$$

$$\therefore \frac{\eta}{R} = \frac{1}{g} \sum_{i=1}^{\infty} \frac{2}{\varepsilon_i^2 - 1} \frac{J_1(\varepsilon_i \frac{r}{R})}{J(\varepsilon_i)} (\alpha_i - \alpha_g) \cos\theta \tag{9}$$

where

$\alpha_i = \dot{v}_i$ = nominal acceleration response of liquid

The liquid pressure response p is given as follows by using eq. (5).

$$p = \frac{\gamma_f}{g} \frac{\partial \phi}{\partial t}$$

$$= \gamma_f H \frac{1}{g(\frac{H}{R})} \sum_{i=1}^{\infty} \frac{2}{\varepsilon_i^2 - 1} \frac{J_1(\varepsilon_i \frac{r}{R})}{J_1(\varepsilon_i)} \left\{ \frac{\cosh(\varepsilon_i \frac{z}{R})}{\cosh(\varepsilon_i \frac{H}{R})} \alpha_i - \alpha_g \right\} \cos\theta$$

$$\therefore \frac{p}{\gamma_f H} = \frac{1}{g(\frac{H}{R})} \sum_{i=1}^{\infty} \frac{2}{\varepsilon_i^2 - 1} \frac{J_1(\varepsilon_i \frac{r}{R})}{J_1(\varepsilon_i)} \left\{ \frac{\cosh(\varepsilon_i \frac{z}{R})}{\cosh(\varepsilon_i \frac{H}{R})} \alpha_i - \alpha_g \right\} \cos\theta \tag{10}$$

where γ_f denotes the weight of liquid per unit volume.

Therefore, the side wall pressure p_w and the bottom pressure p_b are given as follows.

$$\frac{p_w}{\gamma_f H} = \frac{p}{\gamma_f H}\Bigg|_{r=R}$$

$$= \frac{1}{g\left(\frac{H}{R}\right)} \sum_{i=1}^{\infty} \frac{2}{\varepsilon_i^2 - 1} \left\{ \frac{\cosh\left(\varepsilon_i \frac{z}{R}\right)}{\cosh\left(\varepsilon_i \frac{H}{R}\right)} \alpha_i - \alpha_g \right\} \cos\theta \qquad (11)$$

$$\frac{p_b}{\gamma_f H} = \frac{p}{\gamma_f H}\Bigg|_{z=0}$$

$$= \frac{1}{g\left(\frac{H}{R}\right)} \sum_{i=1}^{\infty} \frac{2}{\varepsilon_i^2 - 1} \frac{J_1\left(\varepsilon_i \frac{r}{R}\right)}{J_1(\varepsilon_i)} \left\{ \frac{1}{\cosh\left(\varepsilon_i \frac{H}{R}\right)} \alpha_i - \alpha_g \right\} \cos\theta \qquad (12)$$

Next, the resultant force in x-direction F_x is calculated as follows by using side wall pressure p_w.

$$F_x = \int_0^{2\pi} \int_0^H \left(p_w R \, d\theta \, dz \right) \cos\theta$$

$$= W_f \frac{1}{g} \sum_{i=1}^{\infty} \frac{2}{\varepsilon_i^2 - 1} \left\{ \frac{\tanh\left(\varepsilon_i \frac{H}{R}\right)}{\varepsilon_i \frac{H}{R}} \alpha_i - \alpha_g \right\} \cos\theta$$

$$\therefore \frac{F_x}{W_f} = \frac{1}{g} \sum_{i=1}^{\infty} \frac{2}{\varepsilon_i^2 - 1} \left\{ \frac{\tanh\left(\varepsilon_i \frac{H}{R}\right)}{\varepsilon_i \frac{H}{R}} \alpha_i - \alpha_g \right\} \cos\theta \qquad (13)$$

where $W_f (= \pi R^2 H \gamma_f)$ means the total weight of liquid contained in the vessel.

Turning moment about y-axis due to the side wall pressure p_w is calculated as follows.

$$M_w = \int_0^{2\pi} \int_0^H z \left(p_w R \, d\theta \, dz \right) \cos\theta$$

$$= W_f \frac{H}{2} \frac{1}{g} \sum_{i=1}^{\infty} \frac{4}{\varepsilon_i^2 - 1} \left[\frac{\tanh\left(\varepsilon_i \frac{H}{R}\right)}{\varepsilon_i \frac{H}{R}} \left\{ 1 - \frac{\tanh\left(\frac{\varepsilon_i}{2} \frac{H}{R}\right)}{\varepsilon_i \frac{H}{R}} \right\} \alpha_i - \frac{1}{2} \alpha_g \right]$$

$$\therefore \frac{M_w}{W_f \frac{H}{2}} = \frac{1}{g} \sum_{i=1}^{\infty} \frac{4}{\varepsilon_i^2 - 1} \left[\frac{\tanh\left(\varepsilon_i \frac{H}{R}\right)}{\varepsilon_i \frac{H}{R}} \left\{ 1 - \frac{\tanh\left(\frac{\varepsilon_i}{2} \frac{H}{R}\right)}{\varepsilon_i \frac{H}{R}} \right\} \alpha_i - \frac{1}{2} \alpha_g \right] \qquad (14)$$

Turning moment about y-axis due to the bottom pressure p_b is also calculated as follows.

$$M_b = \int_0^{2\pi} \int_0^{R} (p_b \, r \, d\theta \, dr) \, r \cos\theta$$

$$= W_f \frac{H}{2} \frac{1}{g\left(\frac{H}{R}\right)^2} \sum_{i=1}^{\infty} \frac{4}{\varepsilon_i^2 - 1} \left\{ \frac{1}{\cosh\left(\varepsilon_i \frac{H}{R}\right)} \alpha_i - \alpha_g \right\}$$

$$\therefore \frac{M_b}{W_f \frac{H}{2}} = \frac{1}{g\left(\frac{H}{R}\right)^2} \sum_{i=1}^{\infty} \frac{4}{\varepsilon_i^2 - 1} \left\{ \frac{1}{\cosh\left(\varepsilon_i \frac{H}{R}\right)} \alpha_i - \alpha_g \right\} \qquad (15)$$

Actual turning moment about y-axis is given as the sum of M_w and M_b as follows.

$$\frac{M_y}{W_f \frac{H}{2}} = \frac{M_w}{W_f \frac{H}{2}} + \frac{M_b}{W_f \frac{H}{2}} \qquad (16)$$

3.2 Period of Sloshing of Lqiuid

As already known in the papers by Housner and so on, the period of sloshing of liquid of i-th order T_i is given as follows by using eq. (7).

$$T_i = \frac{2\pi}{\omega_i} = 2\pi \sqrt{\frac{R}{g} \frac{\coth\left(\varepsilon_i \frac{H}{R}\right)}{\varepsilon_i}} \qquad (17)$$

As an example of calculation, the periods of sloshing of liquid in about 100×10^3 kℓ cylindrical oil storage (D=80m, H=20m) are shown in Tab. 3.

Tab. 3 Periods of sloshing of liquid in 100x10^3 kl cylindrical oil storage

i	T_i (sec)	i	T_i (sec)
1	10.978	6	2.991
2	5.524	7	2.759
3	4.346	8	2.575
4	3.710	9	2.423
5	3.292	10	2.294

The period of sloshing of liquid of the first order is the most significant of all and is given as follows.

$$T_1 = 4.63 \sqrt{\frac{R}{g} \coth\left(1.84 \frac{H}{R}\right)} \tag{18}$$

The eq. (18) is used so frequently in the design of cylindrical liquid storage that a nomogram to calculate it availably was made. This is shown in Fig. 19. In this figure, the periods of sloshing of liquid in variable storages now in use are also plotted. It is found, from this figure, that the period of sloshing in storages now in use ranges up to 12 sec.

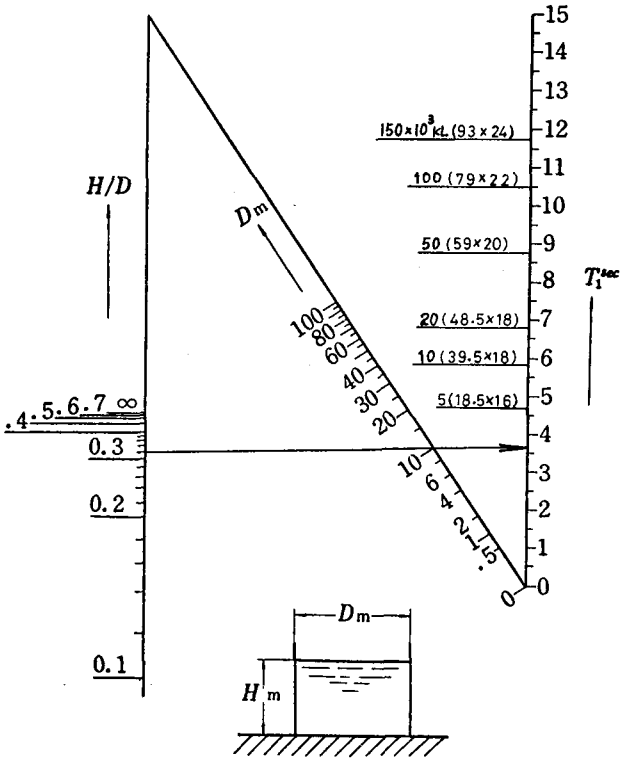

Fig. 19 Period of Sloshing of Liquid of the First Order

3.3 Response of the First Order

It is the response of the first order of all that has the most significance in the sense of aseismic design. This is thought to give the direct effect by which the liquid overflows from the

side wall and the vessel is broken by the effect of pressure. In this section, the discussion is made for the response of the first order.

The response of the first order is given by taking the first term of summation of eq. (9) ∿ (16). The mode of response of the first order is illustrated in Fig. 20. So the maximum amplitude of each response is given as follows.

Liquid displacement h :

$$\theta_h = \frac{h}{R} = \frac{\eta_1}{R}\Bigg|_{\substack{r=R\\ \theta=0}} = 0.837\,\frac{1}{g}\,(\alpha_1 - \alpha_g) \tag{19}$$

Side wall pressure P_w:

$$\frac{P_w}{\gamma_f H} = \frac{p_w}{\gamma_f H}\Bigg|_{\substack{\theta=0\\ z=H}} = 0.837\,\frac{1}{g\left(\frac{H}{R}\right)}(\alpha_1 - \alpha_g) \tag{20}$$

Bottom pressure P_b :

$$\frac{P_b}{\gamma_f H} = \frac{p_b}{\gamma_f H}\Bigg|_{\substack{r=R\\ \theta=0}} = 0.837\,\frac{1}{g\left(\frac{H}{R}\right)}\left\{\frac{1}{\cosh\left(1.84\frac{H}{R}\right)}\alpha_1 - \alpha_g\right\} \tag{21}$$

It should be noted that θ_h also represents the angle of inclination of liquid surface.

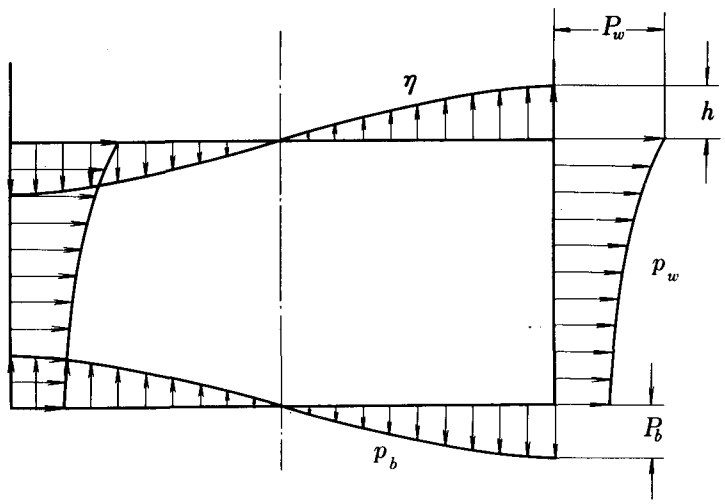

Fig. 20 Mode of Response of the First Order

The response spectrum of θ_h was calculated as an example of response analysis. The eq. (8) was integrated by Runge-Kutta-Gill method to give the response of $\alpha_i (=\dot{v}_i)$. And using this into eq. (19), the response of θ_h was calculated.

Fig. 21 represents the response spectrum of θ_h to the input of El Centro wave whose maximum acceleration is 1.0G .

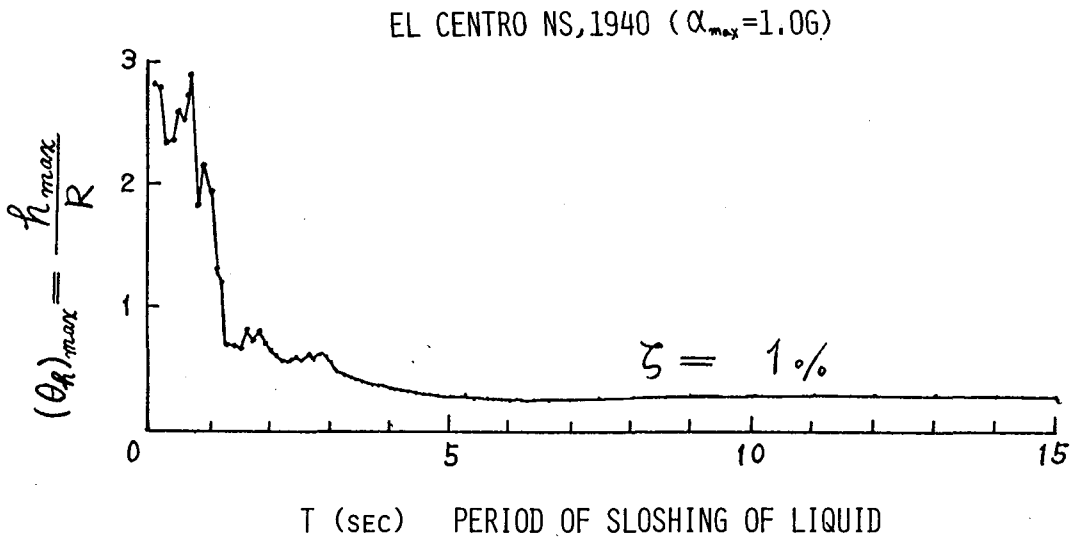

Fig. 21 Response Spectrum of θ_h

It is found, from this figure, that the response spectrum of θ_h is similar to the relative acceleration spectrum of one mass-spring system. The curve of the response spectrum of θ_h becomes flat with the increase of the period of sloshing of liquid.

3.4 Simple Calculation Method for the Response of the First Order

It was shown in section 2.2 that the ground displacement wave which causes the sloshing of liquid is similar to sinusoidal wave and the sloshing response wave is also similar to sinusoidal wave. From this fact, the ground motion can be assumed to be simulated by sinusoidal wave whose period is equal to the period of liquid sloshing of the first order. However, the component of the same period does not continue so long during earthquake that the response does not grow up to the steady state value but decays from a value. It is wanted to know how much the response grows during the earthquake.

To estimate this value availably, a simple calculation method

to use the trangient response to the input of sinusoidal wave was proposed in this section. First, the trangient response to the input of n times of period of sinusoidal wave whose period is equal to the period of liquid sloshing of the first order was calculated. Next, this trangient response was compared with the responses which were obtained as the result of experiment in section 2 and others during earthquake motions. Finally, the author found out the equivalent input wave number of sinusoidal wave n_e at which the trangient response to sinusoidal wave input corresponded to the response to earthquake wave input.

Based on this method, the sloshing response can be availably calculated by using the input of n_e times of sinusoidal wave whose period is equal to the period of liquid sloshing of the first order.

The estimation of the equivalent input wave number of sinusoidal wave n_e was carried out as follows.

By the use of eq. (8) and eq. (19), the maximum response of the liquid displacement at side wall to the input of n times of period of sinusoidal wave whose period is equal to the period of liquid sloshing of the first order, that is

$$d_g(t) = D_g \sin\left(2\pi \frac{t}{T_1}\right) \qquad (0 \leqq t \leqq nT_1) \tag{22}$$

is given as follows.

$$h(n) \simeq 4.84\ D_g \tanh\left(1.84 \frac{H}{R}\right) \tag{23}$$

So the maximum response of the displacement of the center of gravity of liquid is approximately given as follows.

$$x_g(n) \simeq \frac{h(n)}{4\left(\frac{H}{R}\right)} = 1.21\ D_g \frac{\tanh\left(1.84 \frac{H}{R}\right)}{\frac{H}{R}} n \tag{24}$$

Therefore the trangient response factor of the displacement of the center of gravity of liquid to the displacement of the ground motion is given as follows.

$$A_g(n) = \frac{x_g(n)}{D_g} = 1.21 \frac{\tanh\left(1.84 \frac{H}{R}\right)}{\frac{H}{R}} n \tag{25}$$

This is illustrated in Fig. 22. Shaping parameter of the storage H/R is taken as abscissa and the trangient response factor $A_g(n)$ as

ordinate and the input wave number of sinusoidal wave n as parameter.

Furthermore, the response factors of the displacement of the center of gravity of liquid A_g obtained as the result of experiments during earthquake motions are also plotted in this figure. The mark ⊙ represents the response factors A_g obtained as the result of experiment in section 2. And the mark ⊗ represents the response factor A_g obtained as the result of experiment which shakes the model storage of diameter 1.0m on the shaking table to the input of strong earthquake record: El Centro, Taft and so on.

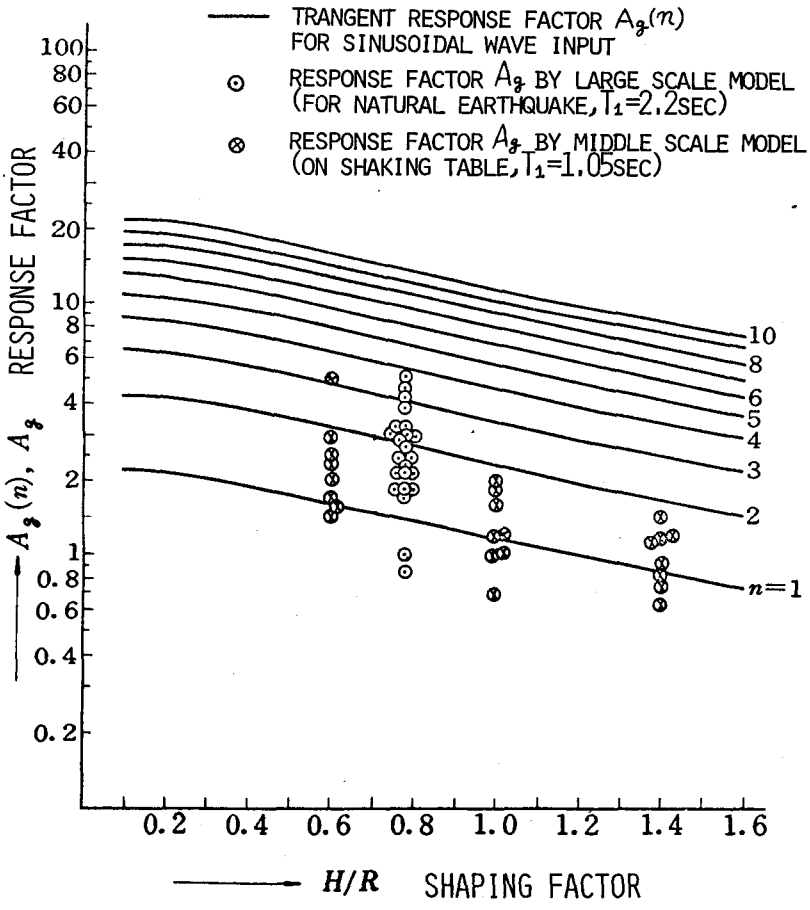

Fig. 22 .Correspondance of Ag(n) and Ag

It is concluded from this figure that the equivalent input wave number of sinusoidal wave is estimated as follows.

$$n_e = 2 \sim 3 \tag{26}$$

For further simplicity of calculation, the author made a nomogram to calculate the maximum response of liquid displacement at side wall availably based on this method. This is illustrated in Fig. 23.

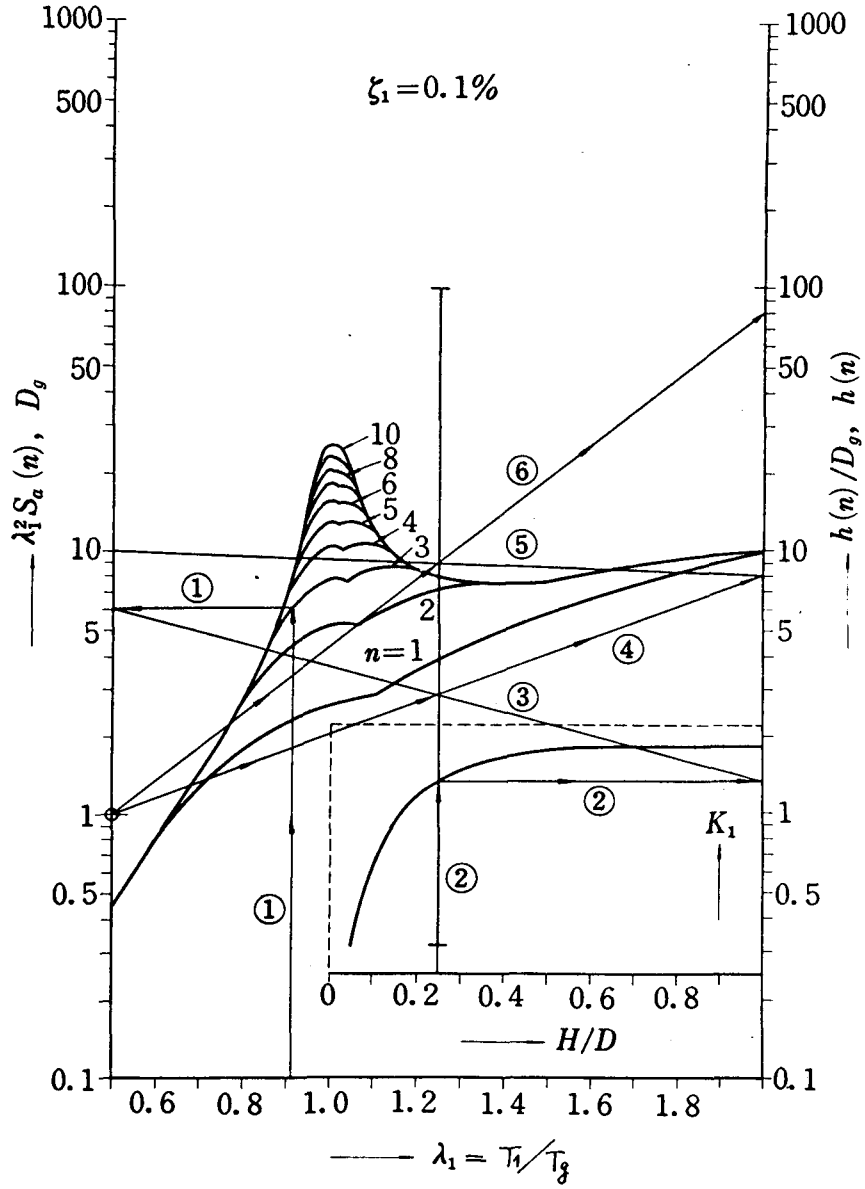

Fig. 23 Nomogram to Calculate the Maximum Displacement of Liquid at Side Wall

4. Response Analysis of Sloshing of Liquid in a Spherical Storage

It is the object in this section to evaluate the basic vibrational characteristics of spherical storage such as the period of sloshing of liquid, ratio of free weight of liquid and so on. First an experiment which shakes the model of spherical vessel on a shaking table was carried out. Next the vibrational characteristics were evaluated based on the result of this experiment by way of simple analysis.

4.1 The Vibrational Model of the Spherical Storage

It makes the analysis of the system easy to separate the vibration of the structure and the vibration of liquid. The system of a spherical storage can be regarded as the connection of a rigid system and a flexible system. The rigid system is composed of the structure and the fixed weight of liquid which gives the inertia force during earthquakes. The flexible system is composed of the free weight of liquid which gives the horizontal force during the sloshing of liquid.

Based on this thought, the system of spherical storage was modeled by a two degrees of freedom system represented in Fig. 24.

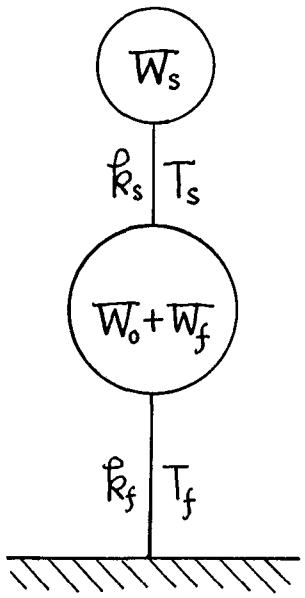

Fig. 24 Vibrational Model

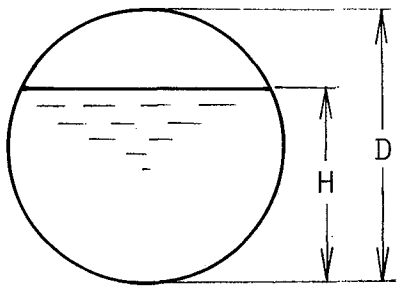

Fig. 25 Depth of Liquid

Notations in Fig. 24 are as follows

W_0 = weight of the structure and the spherical vessel

$W_f = W_w f(h)$ = fixed weight of liquid (27)

$f(h)$ = ratio of fixed weight of liquid

$W_s = W_w S(h)$ = free weight of liquid (28)

$S(h)$ = ratio of free weight of liquid

$W_w = (W_w)_{max} \eta(h)$ = weight of liquid (29)

$(W_w)_{max}$ = full weight of liquid

$\eta(h)$ = ratio of fullness of liquid

T_f = natural period of the structure

T_s = natural period of sloshing of liquid

k_f = spring constant of the structure

k_s = equivalent spring constant of sloshing of liquid

where h denotes the ratio of the depth of liquid and is defined as follows (cf. Fig. 25).

$$h = \frac{H}{D} \tag{30}$$

4.2 Outline of Experiment

An experiment which shakes the model of spherical vessel on a shaking table was carried out to evaluate the basic vibrational characteristics of spherical storage such as the period of sloshing of liquid, ratio of free weight of liquid and so on. The shaking table was actuated to sinusoidal wave and the record of strong earthquake motion. The model of spherical vessel was attached to the shaking table through a spring of high rigidity by which the reaction force of the shaking table was measured. The model of spherical vessel whose diameter is 500 mm was made by transparant plastics so that the sloshing of liquid in the vessel can be observed from outside. The measurement was done for sloshing

displacement of liquid, pressures on vessel, reaction force of the shaking table and the motion of the shaking table. The system for measurement and recording is illustrated in Fig. 26.

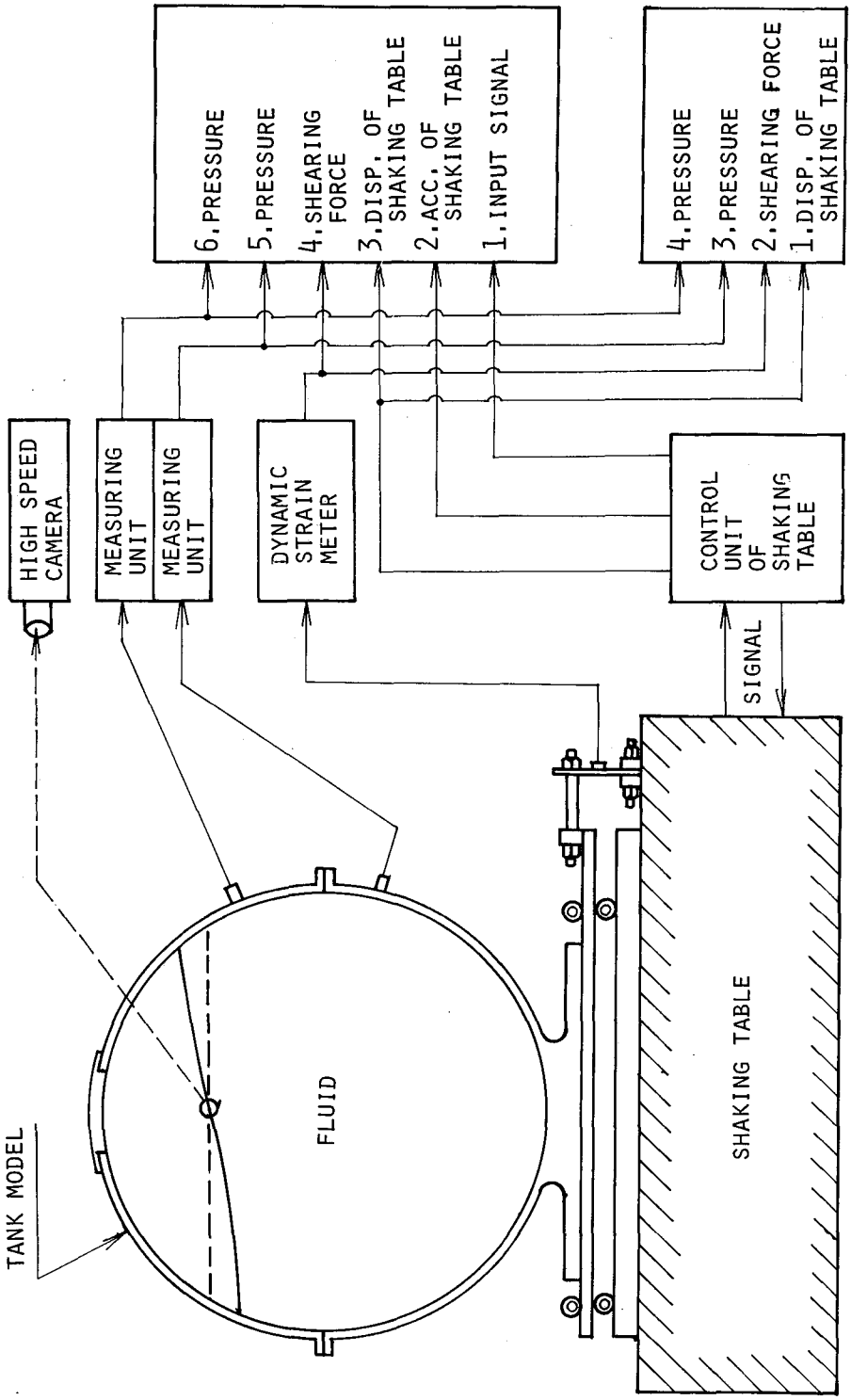

Fig. 26 System for Measurement and Recording

4.3 Patterns of Sloshing of Liquid

The system was shaken at the resonant point of sloshing to the input of sinusoidal wave and the sloshing displacement of the surface of liquid was recorded by using high speed camera. It was found, from the analysis of the record, that the patterns of sloshing of liquid in spherical vessel is so much different from that in cylindrical vessel.

The patterns of sloshing of liquid is represented in Fig. 27 when the parameter h charges from 0.1 to 0.9 by step of 0.2.

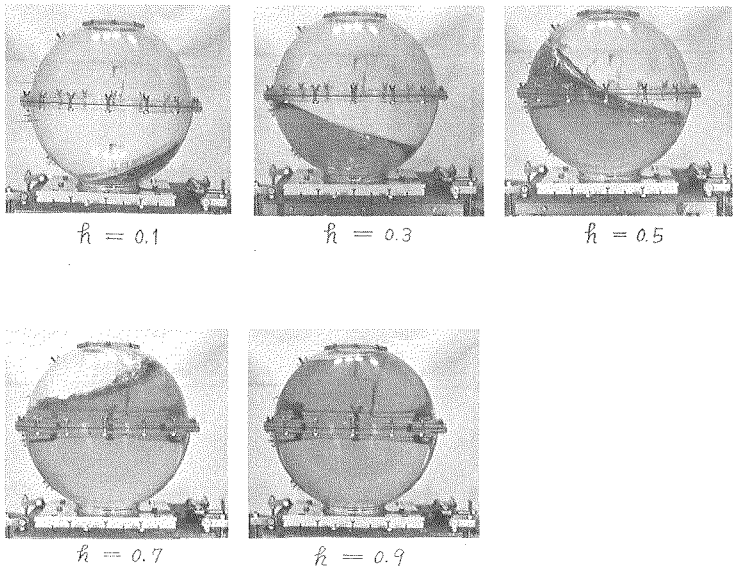

Fig. 27 Sloshing Pattern of Liquid

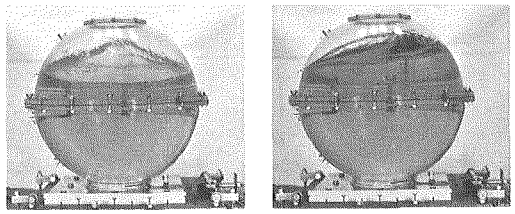

Fig. 28 Rotating Pattern of Liquid

This figure shows that the patterns of sloshing of liquid can be classified into next three.

1) The case that h is less than 0.3

   In this case, the liquid moves along the wall of the vessel holding almost same shape at its rest. Therefore the surface of liquid is almost held as plane. This is the typical pattern which appears in spherical vessel.

2) The case that h is more than 0.3 but less than 0.8

   In this case, the liquid shows complex pattern as the superposition of the first order mode which moves as plane and the higher order mode which moves as ripple. This tendancy is remarkable for around $h=0.65$, where it can not be easily judged whether it is the resonance of the first order or the higher order.

3) The case that h is more than 0.8

   In this case, the edge of liquid moves along the wall of the vessel. The surface of liquid is almost held as plane but is more disturbed than the case that h is less than 0.3. This is also the typical pattern which appears in spherical vessel.

In addition to these three patterns of sloshing, the rotating pattern of liquid was observed. The examples of this pattern are shown in Fig. 28. This pattern appears remarkably when the amplitude of sloshing is large. It continues for a long time if it appears. This is thought to be caused by the disturbance of liquid because it does not appear when the amplitude of liquid sloshing is small and the liquid is not disturbed.

4.4 Period of Sloshing of Liquid

First, an experiment which shakes the model of spherical storage was made to evaluate the period of sloshing of liquid. Next an semi-experimental formula to approximate the result of this experiment was made by way of simple analysis. Finally the result of this analysis was illustrated into a nomogram to evaluate the period of sloshing of liquid in a spherical storage availably.

The result of the experiment is shown in Fig. 29. The mark ⊗ represents the value obtained as the result of the experiment which was carried out in our laboratory using the model of diameter 0.5m. The mark ○ represents the value given by the result of an experiment which was carried out by Akiyama using a model of diameter 6.0m. It is found that the both show a good agreement in spite of the difference of diameter.

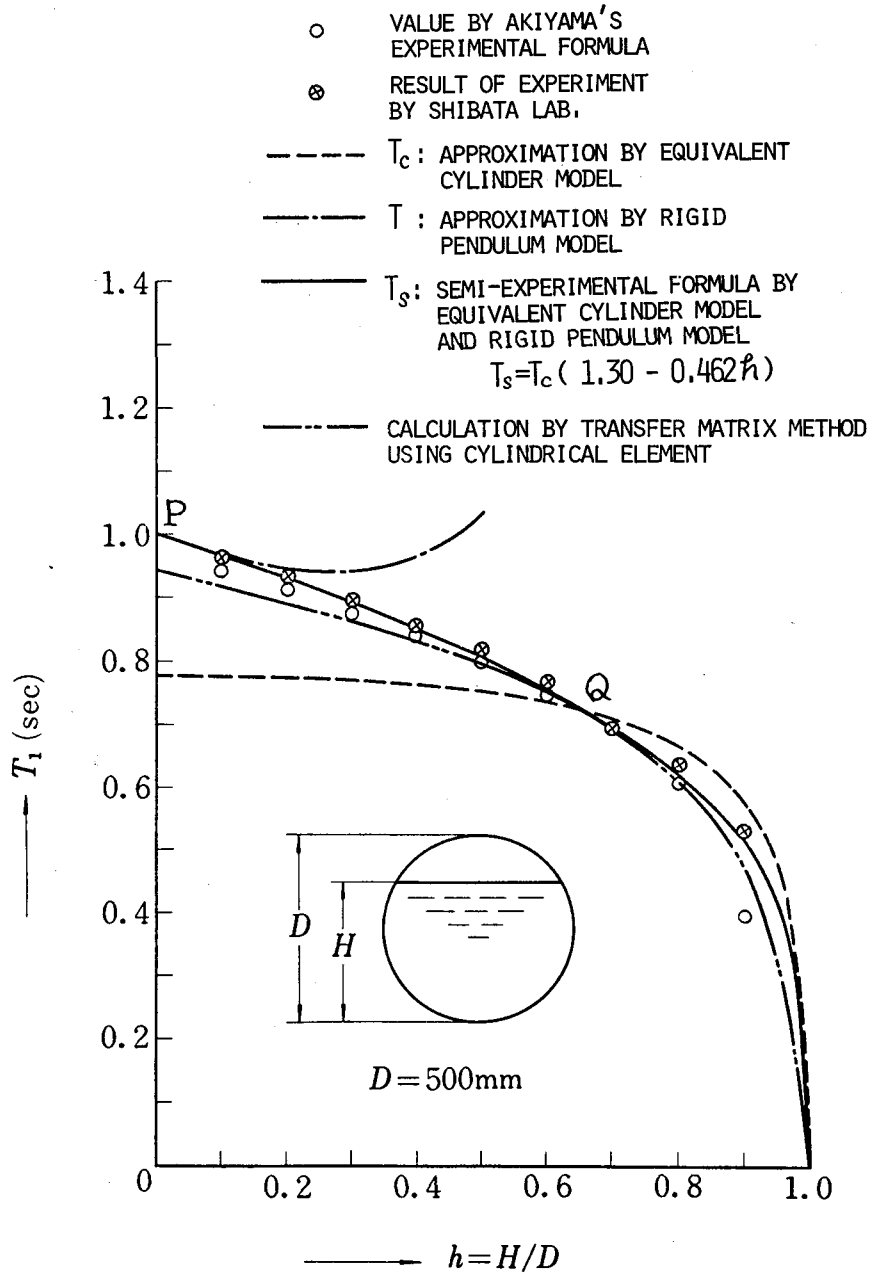

Fig. 29 Period of Sloshing of Liquid

Next, the period of sloshing was estimated when the liquid was very little. It is obtained from the result of the experiment shown in section 4.3 that liquid moves along the wall of the vessel holding almost the same shape at its rest when the liquid is very

little. So the motion of liquid in this case can be modeled by a rigid pendulum model illustrated in Fig. 30.

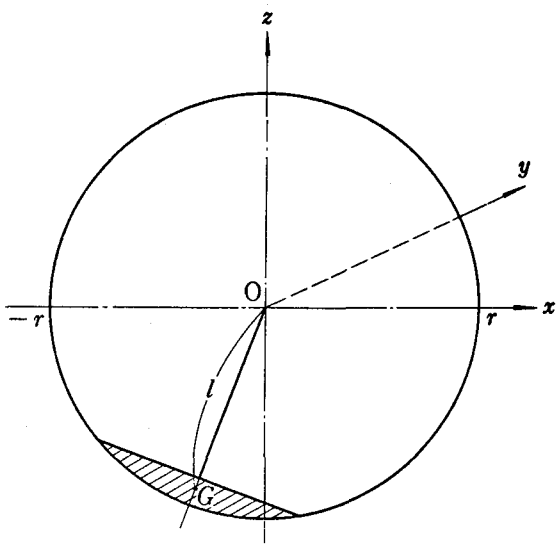

Fig. 30 Rigid Pendulum Model

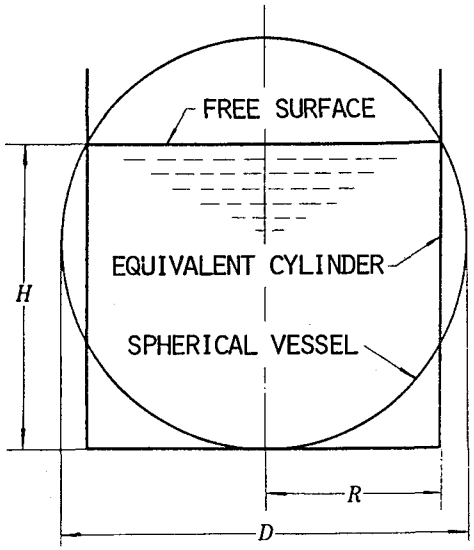

Fig. 31 Equivalent Cylinder Model

The period of this model T is given as follows.

$$T = 2\pi \sqrt{\frac{D}{2g}} \sqrt{\frac{60 - 160h + 180h^2 - 72h^3}{60(1-h)^2}} \qquad (31)$$

The result of this analysis is illustrated in Fig. 29 by the curve ——·—— . It shows that this approximates the result of experiment well when the liquid is little. This curve crosses the ordinate at point P, whose value is $2\pi\sqrt{D/2g}$.

Next, the spherical vessel was approximated by a cylindrical vessel which circumscribed the surface of liquid. This is illustrated in Fig. 31. The period of sloshing of liquid in this cylindrical vessel T_c is given as follows.

$$T_c = T_{co}\, S_c\,(h) \qquad (32)$$

where

$$T_{c0} = 2\pi \sqrt{\frac{D}{2g}}\ \frac{\sqrt{2}}{1.84} \qquad (33)$$

$$S_c(h) = \sqrt{1.84\sqrt{h(1-h)}\ \coth\left(1.84\sqrt{\frac{h}{1-h}}\right)} \qquad (34)$$

The value of T_c is illustrated in Fig. 29 by the curve -----. This figure shows that the feature of this curve is similar to the result of experiment and the both cross each other at point Q where h is around 0.65.

As the result of this fact, the author assumed that the form of semi-experimental formula which approximates the period of slowshing of liquid in a spherical storage is given as follows.

$$T_s = T_c\ (\alpha + \beta h) \qquad (35)$$

The coefficient α and β were determined so that the curve of T_s passed the points P and Q . Finally, T_s were determined as follows.

$$T_s = T_c\ (1.30 - 0.462\,h) \qquad (36)$$

The value of T_s is illustrated in Fig. 29 by the curve ———. It shows that T_s approximates the result of experiment well. The curve —·—·— in Fig. 29 illustrates the value of the period of sloshing of liquid in a spherical storage calculated by theoretical analysis using transfer matrix method.

Finally a nomogram to calculate the period of sloshing of liquid in spherical and cylindrical storages was made. This is illustrated in Fig. 32. It is found from this figure that the period of sloshing of liquid in a spherical storage changes more than that of cylindrical storage in accordance with the change of the depth of liquid h .

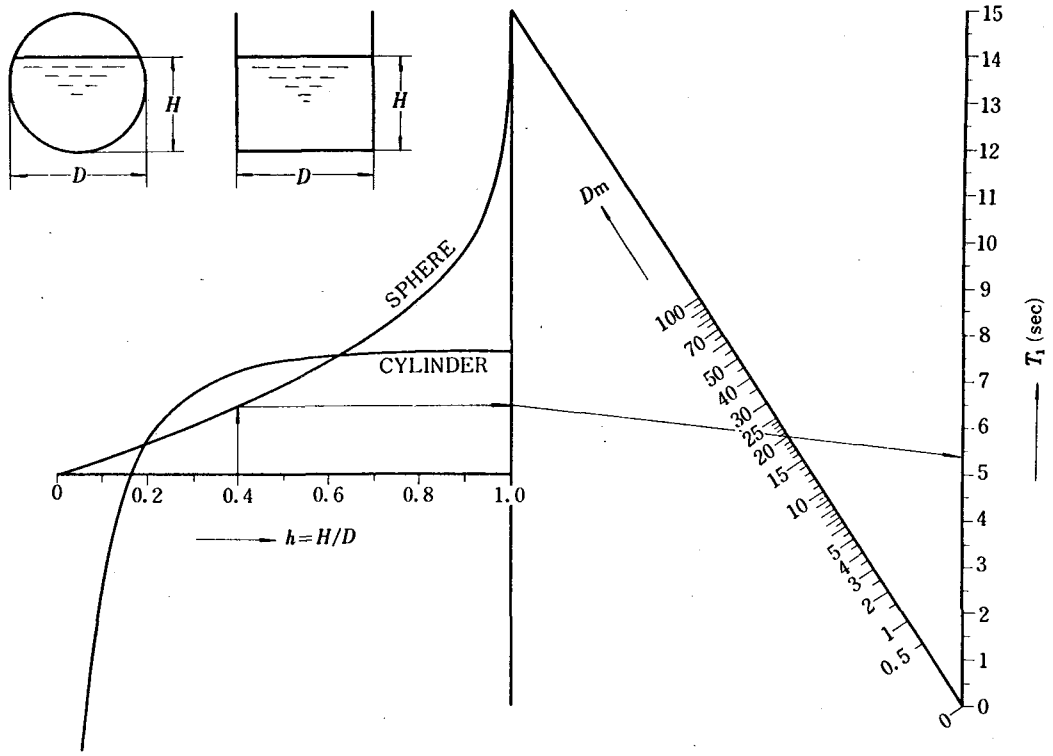

Fig. 32 Period of Sloshing of Liquid

4.5 The Ratio of Free Weight of Liquid

In this section the ratio of free weight of liquid was obtained as the result of an experiment which shakes the model of spherical storage to the input of sinusoidal wave.

Assume the system illustrated in Fig. 24 accepts the input of n times of period of sinusoidal wave whose period is equal to the period of sloshing of liquid T_s, the maximum response of the base shear force $Q(n)$ is given as follows.

$$Q(n) = \pi \frac{W_s}{g} \alpha_g n \quad (37)$$

where α_g denotes the maximum acceleration of the ground motion and is given by

$$\alpha_g = D_g \omega_g^2 = D_g \left(\frac{2\pi}{T_s}\right)^2 \quad (38)$$

Therefore, if the maximum response of the base shear force $Q(n)$ and the maximum acceleration of the ground motion α_g are measured, the

free weight of liquid is calculated by

$$W_s = Q\ (n)\ \frac{g}{\pi \alpha_g n} \tag{39}$$

and the ratio of free weight of liquid can be calculated as follows.

$$S\ (h) = \frac{W_s}{W_w} \tag{40}$$

Based on this way, the ratio of free weight of liquid was obtained experimentally. The result is illustrated in Fig. 33.

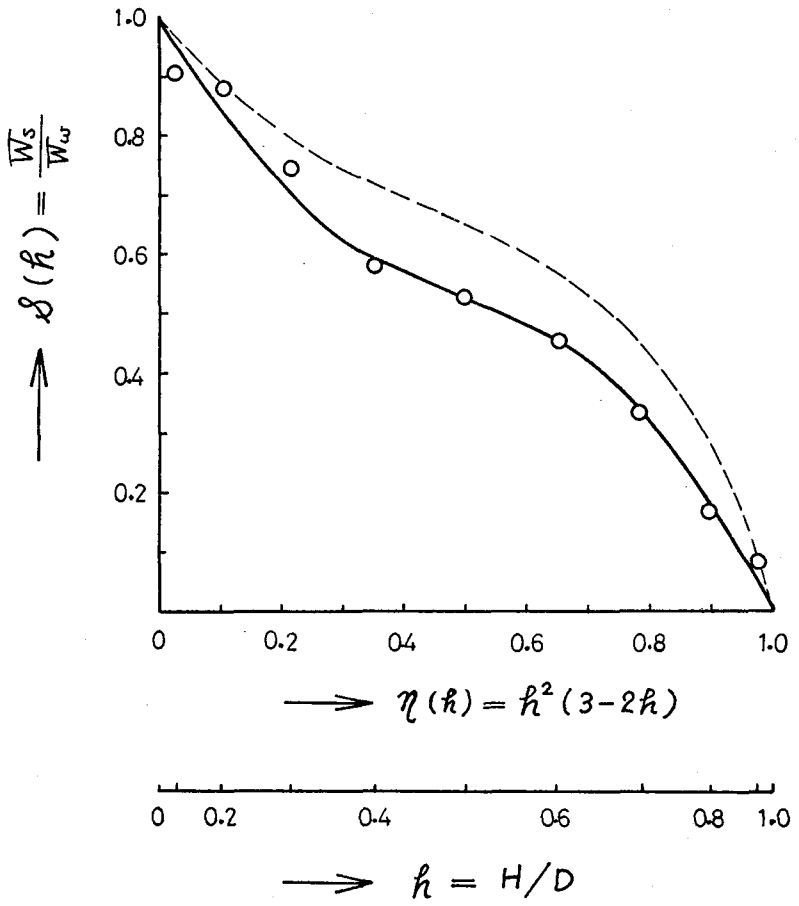

Fig. 33 The Ratio of Free Weight of Liquid

4.6 Base Shear Force

In this section the base shear force by sloshing of liquid in a spherical storage is evaluated by using the result of the ratio of free weight of liquid obtained in section 4.5.

It was shown in section 3.4 that the response of sloshing of liquid in the cylindrical storage during earthquake is estimated by the trangient response to the input of n_e times of period of sinusoidal wave whose period is equal to the period of sloshing of liquid. It is assumed in this section that this is also applicable for the spherical storage.

The maximum response of base shear force $Q(n)$ when the system accepts n times of period of sinusoidal wave whose period is equal to the period of sloshing of liquid is given by eq. (37). By the use of eqs. (28) and (29), eq. (37) is modified into next form.

$$Q(n) = (W_w)_{max} K_g n \cdot \pi \eta(h) S(h) \tag{41}$$

where K_g denotes the seismic coefficient of the ground motion.

Here the coefficient of base shear force $q(h)$ is defined as follows.

$$q(h) = \frac{Q(n)}{(W_w)_{max} K_g n} = \pi \eta(h) S(h) \tag{42}$$

This means the maximum response of base shear force per unit volume of liquid when the system accepts the input of one time of period of sinusoidal wave whose maximum acceleration is 1.0G.

This was calculated by using the result of free weight of liquid given in Fig. 33, and was illustrated in Fig. 34.

It is found from this figure that $q(h)$ gives its maximum value at $h \simeq 0.6$.

Finally, when the spherical tank accepts the input of n times of period of sinusoidal wave whose seismic coefficient is K_g, the maximum response of the base shear force $Q(n)$ is evaluated as follows.

$$Q(n) = (W_w)_{max} K_g \, q(h) \, n \tag{43}$$

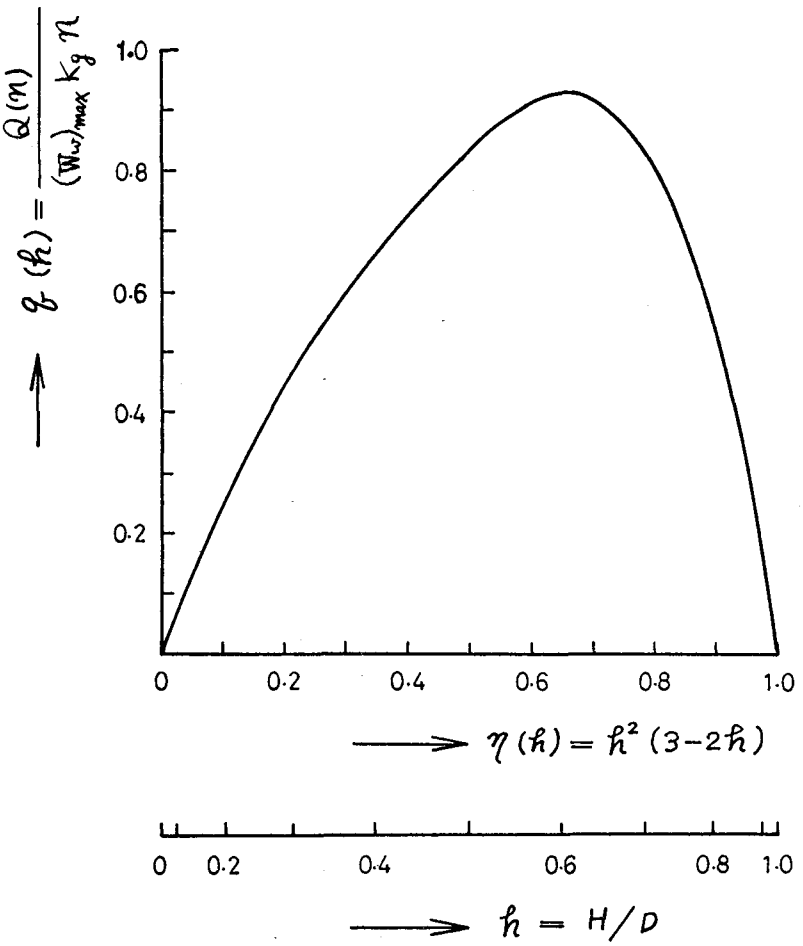

Fig. 34 Shearing Force Coefficient to Sinusoidal Wave Input

5. Concluding Remarks

The author made clear the fundamental vibrational characteristics of sloshing of liquid in cylindrical and spherical vessels to evaluate the sloshing effects of liquid. The results are illustrated in charts which are available for the response calculation of sloshing of liquid in the aseismic design of cylindrical and spherical storages.

6. Acknowledgements

The author would like to express his appreciation to Professor H. Shibata, the Institute of Industrial Science, University of Tokyo, for his continuous instruction and also to the members in Shibata laboratory for their valuable assistances and discussions.